Seventh International Conference on Computational Fluid Dynamics (ICCFD7), Big Island, Hawaii, July 9-13, 2012

ICCFD7-4403

Numerical Study on Leading Edge Receptivity of the Flat Plate Boundary Layer to Vortical Disturbance

Y. Nishio*, M. Shigeta*, S. Izawa* and Y. Fukunishi*
Corresponding author: nishio@fluid.mech.tohoku.ac.jp

* Tohoku University, Japan

Abstract: The leading edge receptivity to vorticity disturbance is investigated by a three-dimensional numerical simulation. The disturbances are given by a two dimensional periodic vorticity fluctuation at the upstream boundary as a boundary condition. The vorticity fluctuation inside the boundary layer becomes more intense when the vertical scale of the oncoming vorticity fluctuation is larger. It is shown that the tangential velocity induced at the stagnation point is crucial to the leading edge receptivity.

Keywords: Receptivity, Elliptic Leading Edge, Vorticity.

1 Introduction

Laminar-turbulent transition under a low-disturbance environment starts from the amplification of minute velocity disturbances in a boundary layer. The disturbances generally originate from a freestream, entering the boundary layer around the leading edge, where the receptivity is the highest The boundary layer receptivity has attracted a number of researchers for several decades[1-3] because it is the crucial part of the transition process. Kendall[4] showed the relation between freestream turbulences and T-S waves in the boundary layer by a wind tunnel experiment. Dovgal et al.[5] also performed a wind tunnel experiment to investigate the response of a boundary layer to periodic disturbances in the freestream using an oscillating ribbon set upstream of a flat plate. However, the experimental approach has its limits because the thickness of the boundary layer in the vicinity of the leading edge is too thin to measure the velocity or vorticity. Recently, Lars-Uve Schrader et al.[6] discussed the receptivity of a flat plate with an elliptic leading edge using a numerical simulation. Their results indicate the importance of the stretching and tilting of vertical or axial vortices at the leading edge. In this study, the leading edge receptivity against incoming vortical disturbances is numerically investigated, focusing on the deformation of vorticity patterns inside a boundary layer.

2 Numerical Method

Three-dimensional unsteady incompressible Navier-Stokes equations and the continuity equation are solved by the finite difference method using a body-fitted coordinate on a regular grid system. A third-order upwind difference scheme is used in the convection terms written in a gradient form. For the other terms, the second-order central difference scheme is employed. The third-order Adams-Bashforth explicit scheme is used for the convection term and the Crank-Nicolson implicit scheme is applied to the viscous term. In addition, the multi-directional finite different scheme is used for the discretization of the all terms in the N-S equations. Figure 1 shows the computational domain around a flat plate with an elliptic leading edge of an aspect ratio of 1:5, where a is the leading edge length and b is the half of the thickness of the flat plate. The origin of the Cartesian coordinate system is set at the tip of the leading edge of the plate, where x, y and z axes denote the streamwise, vertical and spanwise directions, respectively. The numbers of grids are 449 points in ξ direction, 193 points in η direction, and 6 points in ζ direction. More than 10 grid points are inside the boundary layer at the vicinity of the leading edge at x/a = 0.02. The flat plate length is four times larger than the length of the leading edge. Reynolds number based on the leading edge length a and the freestream velocity U_∞ is 4.0×10^4. The spanwise length of the calculation region is b.

As for the velocity boundary conditions, the non-slip condition is imposed at the wall, the Sommerfeld radiation condition is applied at the outlet boundary and the Dirichlet condition is enforced at the upper and lower boundaries. As for the pressure boundary conditions, the Neumann condition is used at all boundaries and at the wall. The pressure averaged over the calculation field is adjusted to be unity. After the base flow becomes steady, two-dimensional disturbances are added to the freestream by changing only the streamwise velocity u periodically at the upstream boundary. The following equation describes the disturbance,

$$\frac{u'}{U_\infty} = \begin{cases} A\times\sin(2\pi ft)\times(1+0.5/\alpha)\dfrac{s}{y}\left(1-\exp\left(-\alpha\left(\dfrac{y}{s}\right)^2\right)\right) & -\dfrac{l_y}{2}\le\dfrac{y}{a}\le\dfrac{l_y}{2} \\ 0 & \text{otherwise} \end{cases}$$

where f is the non-dimensional frequency, l_y is the length of the oscillation region, A is the amplitude, α is the Lamb-Oseen constant which is 1.25643[7], and s is the parameter corresponding to the vortex core radius. Also, t is the time and t = 0 indicates the moment the disturbance was added. In this study, the simulations are performed for three different scales of s/b, which are 1, 2 and 3. The amplitude of the introduced fluctuation A is 1% of the freestream velocity and the non-dimensional frequency f is 1.

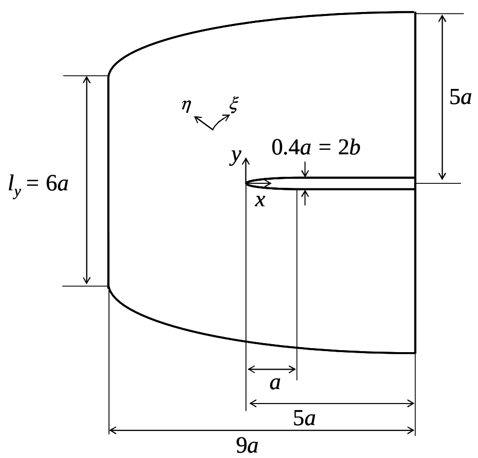

Figure 1 Computational domain

3 Results and Discussion

Vorticity distributions at t =14.0 are shown in Fig. 2. Periodic vorticity patterns can be observed upstream. The vorticity sizes depend on the scale of the vortex core radius s. Figure 3 shows the fluctuations of the spanwise vorticity ω_z at y/a = 0; right upstream of the leading edge. In Fig. 3, the waves appear very similar to each other, even though their vertical scales are different as was shown in Fig.2. The RMS values of the velocity fluctuations in the wall-tangential direction measured at the grid points next to the wall are plotted in Fig.4. There is a noticeable difference between the $u'_{\rm rms}$ at the stagnation point depending on s/b. It should be noted that $u'_{\rm rms}$ at the stagnation point corresponds to the v component velocity there. The velocity fluctuations decay downstream. In particular, they rapidly decay near the leading edge because of the curvature of the round front edge and the favorable pressure gradient. Figure 5 depicts the RMS values of the vertical velocity fluctuations v'_{rms} in the freestream along the y/a = 0 line. The v'_{rms} at the point next to the stagnation point in this figure corresponds to the u'_{rms} there in Fig.4. The periodic waviness in v'_{rms} is caused by the timing of the vortices come in from the upstream boundary. It can be found that the v'_{rms} reaches its peak very close to the leading edge just before it is damped by viscosity. It is also shown that v'_{rms} is influenced by the vortex core radius s. Figure 6 shows the velocity fluctuations u'_{rms} in the boundary layer at x/a = 4.6 together with the averaged velocity profile in the boundary layer at the same location. The velocity fluctuation near the wall becomes higher as the scale of oncoming vorticity fluctuations becomes larger. In this paper, a receptivity coefficient K is defined as the ratio of the amplitude of velocity fluctuations in the boundary layer at lower peak of x/a = 4.6 to that at the upstream boundary which is 1% of the freestream velocity. The results are shown in Table 1. The value of K becomes larger in proportion to the scale parameter s, which is the same tendency as in Fig.6. These results imply that the leading edge receptivity is governed by the periodic tangential velocity fluctuations at the stagnation point.

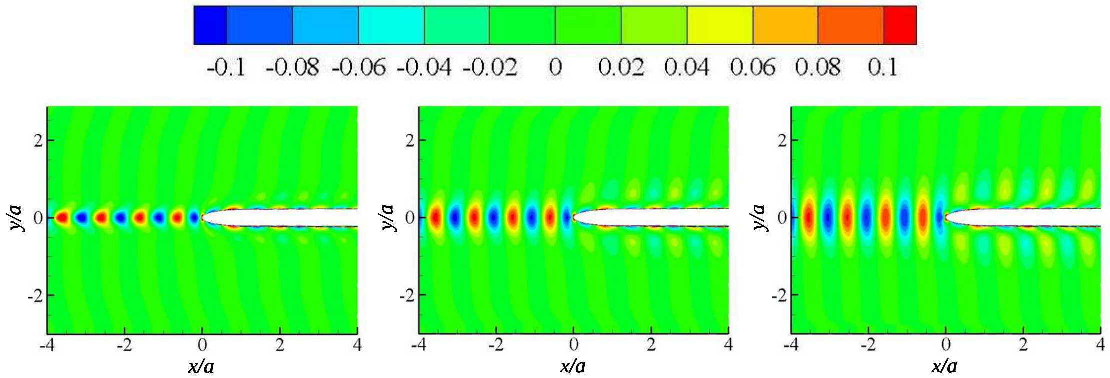

(a) s/b = 1 (b) s/b = 2 (c) s/b = 3

Figure 2 Contour maps of vorticity fluctuation at t = 14.0 for different disturbance scales

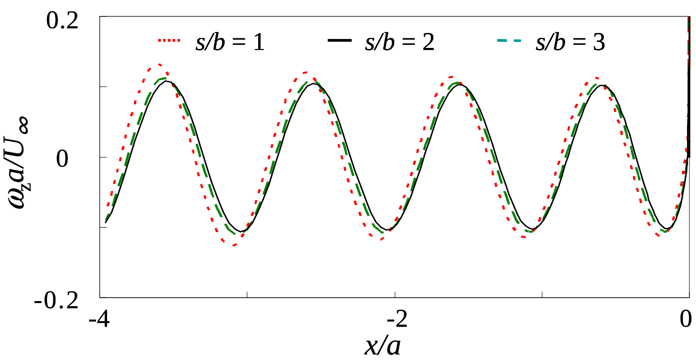

Figure 3 Variation of spanwise vorticity upstream of the leading edge at t = 14.0

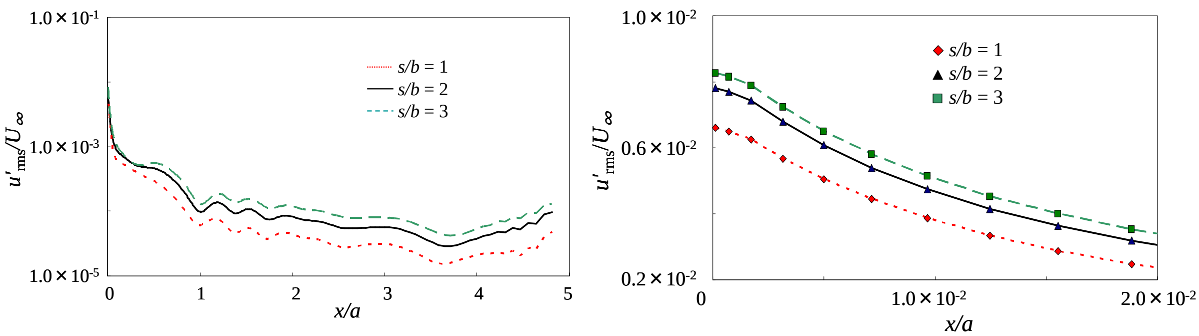

(a) Whole distribution (b) Vicinity of the stagnation point

Figure 4 Distribution of the tangential velocity fluctuations near the wall

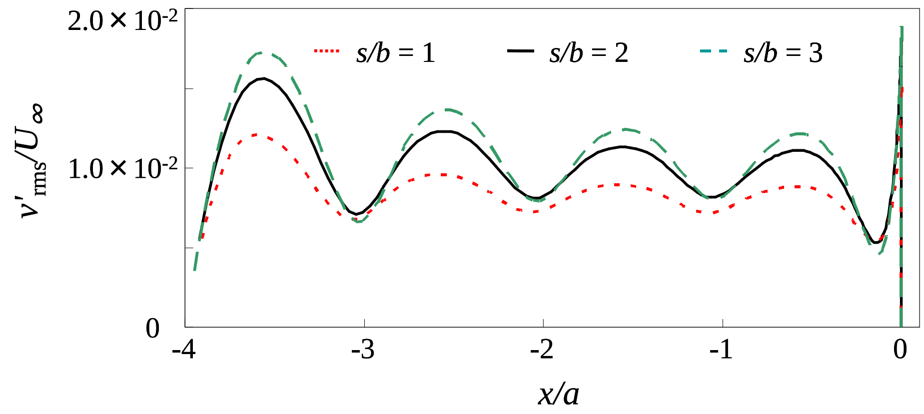

(a) Whole distribution

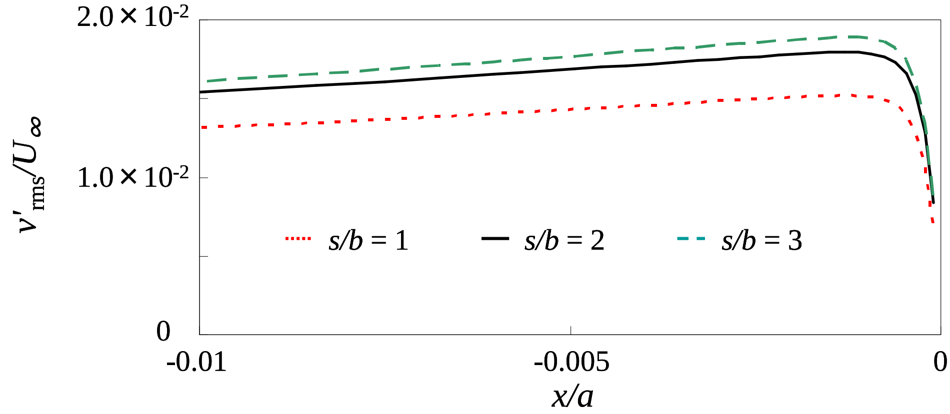

(b) Vicinity of the stagnation point

Figure 5 Distribution of the vertical velocity fluctuations in the freestream along y =0

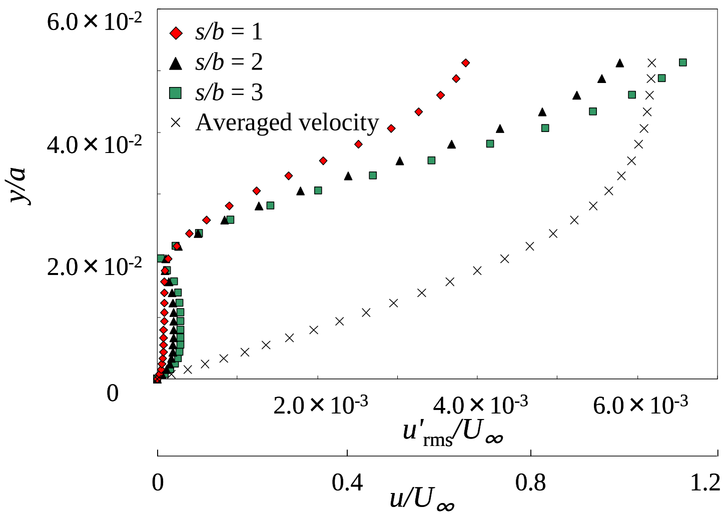

Figure 6 Profiles of velocity fluctuations in the boundary layer at x/a = 4.6

Table 1 Receptivity coefficients at the lower peak of x/a = 4.6

s/b	u'_∞/U_∞	u'_{rms}/U_∞	K
1	0.01	1.41×10^{-4}	1.41×10^{-2}
2	0.01	2.03×10^{-4}	2.03×10^{-2}
3	0.01	2.93×10^{-4}	2.93×10^{-2}

4 Conclusion

A numerical study is performed to investigate a relation between the vorticity disturbances and the leading edge receptivity. Freestream disturbances are given as a two dimensional periodic vorticity fluctuation at the upstream boundary. The result shows that the velocity fluctuation inside a boundary layer becomes more intense when the vertical scale of the oncoming vorticity fluctuation is large. It is found that the tangential velocity fluctuations near the wall at the stagnation point strongly affect the amplitude of velocity fluctuations inside a downstream boundary layer.

References

[1] E. Reshotko, Boundary-layer stability and transition, Annual Review of Fluid Mechanics 9:311-349, 1976

[2] E.J. Kerschen, Boundary Layer Receptivity, AIAA Paper 89-1109:1-10, 1989

[3] W.S.Saric, H.L.Reed and E.J.Kerschen, Boundary-Layer Receptivity to Freestream Disturbance, Annual Review of Fluid Mechanics 34:291-319, 2002

[4] J.M. Kendall, Studies on Laminar Boundary-Layer Receptivity to Freestream Turbulence Near a Leading Edge, Boundary Layer Stability and Transition to Turbulence ASME FED-114:23-30, 1991

[5] A.V. Dovgal, V.V. Kozlov, and V.Ya. Levchenko, Experimental Investigation into the Reaction of a Boundary Layer to External Periodic Disturbance, Fluid Dynamics 15-4:602-606, 1980

[6] L.-U. Schrader, L. Brandt, C. and Mavriplis, D.S. Henningson, Receptivity to free-stream vorticity of flow past a flat plate with elliptic leading edge, Journal of Fluid Mechanics 653:245-271, 2010

[7] W.J. Devenport, M.C. Rife, S.I. Liapis and G.J. Follin, The Structure and Development of a wing tip vortex, Journal of Fluid Mechanics 312:67-106, 1996